Journal of Hazardous Materials 163 (2009) 73–81

Contents lists available at ScienceDirect

Journal of Hazardous Materials

journal homepage: www.elsevier.com/locate/jhazmat

Adsorption of butyl acetate in air over silver-loaded Y and ZSM-5 zeolites: Experimental and modelling studies

Subhash Bhatia*, Ahmad Zuhairi Abdullah, Cheng Teng Wong

School of Chemical Engineering, Universiti Sains Malaysia, Engineering Campus, 14300, Nibong Tebal, Penang, Malaysia

ARTICLE INFO

Article history:
Received 4 April 2008
Received in revised form 17 June 2008
Accepted 17 June 2008
Available online 22 June 2008

Keywords:
Butyl acetate adsorption
Y and ZSM-5 zeolites
Breakthrough curve
Humidity
Adsorption model

ABSTRACT

Adsorption behaviours of butyl acetate in air have been studied over silver-loaded Y (Si/Al = 40) and ZSM-5 (Si/Al = 140) zeolites. The silver metal was loaded into the zeolites by ion exchange (IE) and impregnation (IM) methods. The adsorption study was mainly conducted at a gas hourly space velocity (GHSV) of 13,000 h^{-1} with the organic concentration of 1000 ppm while the desorption step was carried out at a GHSV of 5000 h^{-1}. The impregnated silver-loaded adsorbents showed lower uptake capacity and shorter breakthrough time by about 10 min, attributed to changes in the pore characteristics and available surface for adsorption. Silver exchanged Y (AgY(IE)) with lower hydrophobicity showed higher uptake capacity of up to 35%, longer adsorbent service time and easier desorption compared to AgZSM-5(IE). The presence of water vapour in the feed suppressed the butyl acetate adsorption of AgY(IE) by 42% due to the competitive adsorption of water on the surface and the effect was more pronounced at lower GHSV. Conversely, the adsorption capacity of AgZSM-5(IE) was minimally affected, attributed to the higher hydrophobicity of the material. A mathematical model is proposed to simulate the adsorption behaviour of butyl acetate over AgY(IE) and AgZSM-5(IE). The model parameters were successfully evaluated and used to accurately predict the breakthrough curves under various process conditions with root square mean errors of between 0.05 and 0.07.

1. Introduction

Volatile organic chemicals (VOCs) are emitted as gases from certain solids or liquids which contain organic compounds. Paints, varnishes, and wax all contain organic solvents, as do many cleaning, disinfecting, cosmetic and degreasing products. All of these products can release organic compounds while using them, and, to some degree, when they are stored. When these organic compounds released to atmosphere, they become a key contributor of smog formation. Smog is hazardous because it decreases visibility.

Adsorbent-based processes for the separation of multicomponent gaseous mixtures are becoming increasingly popular. The new generation of synthetic and more selective adsorbents developed in recent years has enabled the adsorption-based technology to compete successfully with the traditional gas-separation techniques, such as cryogenic distillation [1]. Adsorption technology nowadays is being implemented successfully for its commercial applications in the removal of VOCs. For example, SORBATHENE unit technology, based on the pressure-swing adsorption principle, developed and patented by Dow Chemical Company in 1987, has been installed as an economical alternative for the recovery of VOCs [2].

The adsorbent acts as a separation medium for the process. The primary requirements of an absorbent are the selectivity, in which it determines the preferential adsorption of one or more component based upon equilibrium and/or kinetic mechanisms. Besides, a good adsorbent gave the maximum possible loading of VOC on the adsorbent and it must be chemical and physical stable under various operating conditions. Activated carbons are generally used in many adsorption processes due to their higher adsorption capacity and lower price. However, their regeneration is very difficult because of their thermal and chemical instabilities that may cause significant safety problems [3]. As an alternative to activated carbon, high silica zeolites have several advantages. It is reported that at relatively high humidity, carbon takes up appreciable quantities of moisture thereby limiting their effectiveness for VOC uptake [4]. A part of that, zeolites are inorganic and hence, they can be regenerated in air, subject to flammability considerations. The use of hydrophobic zeolites is attracting more and more attention due to their resistance to high thermal operation and their high adsorption affinity for VOC in humid conditions [4].

The common operating experimental variables in the adsorption studies are the gas flow rate, VOC concentration and the type of VOC. Additional variables are the amount of adsorbent and the

* Corresponding author. Tel.: +604 599 6409; fax: +604 594 1013.
E-mail address: chbhatia@eng.usm.my (S. Bhatia).

0304-3894/$ – see front matter © 2008 Elsevier B.V. All rights reserved.
doi:10.1016/j.jhazmat.2008.06.055

temperature of the adsorbent bed. The presence of moisture in the gaseous stream is likely to affect the adsorption process. For adsorption systems that are well designed and operated, continuous VOC removal efficiencies of greater than 95% are achievable for a variety of solvents [5]. It has been observed that at higher gas flow rate, longer time is needed to reach the steady-state concentration under identical operating conditions. This indicates the overall drop in the adsorption rate at higher flow rate [6,7]. A more detailed analysis has revealed that the heat of adsorption varies strongly with VOC concentration range [8]. However, vent streams with high VOC concentration can be diluted with air or inert gases. Second, the type of model VOC chosen with very high molecular weight compounds (MW ≥ 130) and are characterized by low volatility (boiling point >204 °C) are strongly and readily adsorbed on carbon, making it difficult to be desorbed during regeneration. Conversely, low molecular weight compounds (MW < 45) do not adsorb readily on carbon. Tao et al. [9] proposed hydrophobic zeolite as a promising adsorbent, which is superior to activated carbon due to their resistance to humidity and their non-flammability, the use of hydrophobic molecular sieves such as high silica zeolites are gaining importance for the adsorption of VOC.

Gas stream relative humidity above 50% can affect working adsorption capacity at VOC concentration s below 1000 ppm [10]. Chou and Chiou [11] reported that the capacity of a specified adsorbent to adsorb a particular VOC depends mainly on vapour pressure of the VOC, moisture and temperature of the VOC-laden gas stream. Biron and Evans [12] studied the effect of water vapour on the organic mixture adsorption of cyclohexane, acetonitrile, 2-butanone, *iso*-propanol, *n*-heptane, 1-hexanol, diacetone and methylphosphonate by activated carbon. It was found that the adsorption capacities for the organic mixture decreased with increasing relative humidity. Hydrophobic adsorbent has been intensively investigated for humid VOC adsorption as they can eliminate problems associated with suppressing VOC uptake in the presence of high humidity. Zeolites have some advantages because they are hydrophobic and this property changes with an increase in their Si/Al ratio [4].

Combined adsorption–catalytic combustion is an innovative technology for VOC removal in which, the metal loaded adsorbent can also act as good oxidation catalyst for decomposition of VOC during the desorption process at high temperature [13,14]. The adsorption process of the organic vapour onto the adsorbent will be carried out until saturation and subsequently, the desorption stream at high organic concentration will be effectively oxidized by the same material at high temperature. The presence of suitable active metal in the adsorbent is critical during the desorption process to ensure the success of the combustion of the organic molecules. In the present study, silver-loaded zeolite was selected as the dual function adsorbent–catalyst as the metal is reported to be very effective active component for many VOC combustion catalysts [3,15,16]. The high activity of this metal in the oxidation process is associated with its ability to present at multiple oxidation states (+1 to +3) under the reaction conditions and the easy dissociation of oxygen molecules on surface of this metal [16]. Ag loading at low concentration into zeolites is not expected to significantly influence the adsorption behaviour of organic as the adsorption of organic molecules onto metal sites is not usually favoured as compared to that on high surface area zeolites. However, the presence of Ag in those zeolites is crucial in the catalytic combustion stage of the combined adsorption–catalytic combustion process as this metal can act as a good catalyst for the oxidation process.

The objective of the present research is to obtain the breakthrough curves of butyl acetate as a model VOC in a fixed bed of silver-loaded zeolite adsorbent as the first process of the combined VOC adsorption–catalytic decomposition. A suitable adsorption model to evaluate process parameters from the experimental breakthrough data is also proposed. The adsorption process variables are VOC concentration, gas hourly space velocity (GHSV) and the presence of water vapour in the feed. The simulated breakthrough curves are compared with the experimental one. However, the catalytic combustion during the desorption step is beyond the scope of the present study.

2. Modelling

2.1. Model and its numerical solution

The mass balance for the change of the VOC concentration in the fixed bed column is given as:

{Mass accumulated in the gas phase}

+ {mass adsorbed in the solid phase} = 0

$$\left\{\frac{\partial C}{\partial t} - D_L\frac{\partial^2 C}{\partial L^2} + u\frac{\partial C}{\partial L}\right\} + \left\{\frac{1-\varepsilon}{\varepsilon}\,\rho_p\,\frac{\partial q}{\partial t}\right\} = 0 \tag{1}$$

where D_L is the dispersion coefficient (m^2/s); C is the concentration of VOC (mol/m^3); L is length of adsorbent bed (m), u is gas velocity (m/s), ε is bed void fraction, ρ_p is density of adsorbent (kg/m^3) and q is adsorption capacity (mg/g), respectively.

Eq. (1) can be further simplified by assuming the process as a non-equilibrium surface reaction and since the adsorbent bed in the column is relatively short, the diffusion term can be negligible. The net surface reaction rate is equal to the adsorption rate minus the desorption rate as given in Eq. (2).

$$r = \frac{\partial\theta}{\partial t} = k_a(1-\theta)C - k_d\theta \tag{2}$$

In which,

$$\theta = \frac{q}{q_{max}} \tag{3}$$

where θ is the surface coverage of VOC on adsorbent surface. Substitute the surface coverage term into Eq. (1) and the equation can be rewritten as:

$$\frac{\partial C}{\partial t} = -\mu\frac{\partial C}{\partial L} - \left(\frac{1-\varepsilon}{\varepsilon}\right)\cdot\rho_p\cdot q_{max}\cdot\frac{\partial\theta}{\partial t} \tag{4}$$

In general, the voidage, ε can be defined as volume of the adsorbent bed minus the volume of the adsorbent (based on the weight and density of the adsorbent) used and given as:

$$\varepsilon = LA_s - \frac{W}{\rho_p} \tag{5}$$

$(1-\varepsilon)$ can be expressed as volume of the adsorbent used without voidage and is given as:

$$(1-\varepsilon) = \frac{W}{\rho_p} \tag{6}$$

The conversion factor between solid and gas phase, S can be further expressed by the following relation:

$$S = \frac{q_{max}W}{LA_s - (W/\rho_p)} \tag{7}$$

Substitute the conversion factor between solid and gas phase term into Eq. (4) and the equation can be rewritten as:

$$\frac{\partial C}{\partial t} = -\mu\frac{\partial C}{\partial L} - \frac{\partial\theta}{\partial t}S \tag{8}$$

Considering the adsorbent bed as an entity of n series ($n = 50$) of constant volume units, where the physicochemical conditions

within each unit are identical. It is assumed that the adsorption/desorption process follows the Langmuir model. Let Δt (s) and ΔV (m^3) be the residence time and the gas volume in each unit. At the ith unit and experimental time, t, the concentration change in the solid phase and the gas phase can be determined by a finite difference method.

In solid phase, Eq. (2) is expressed as:

$$\theta_i^{t+\Delta t} = \theta_i^t + [k_a(1-\theta_i^t)C_i^t - k_d\theta_i^t] \cdot \Delta t \quad (9)$$

In gas phase, Eq. (8) is expressed as:

$$C_i^{t+\Delta t} = C_i^t + \frac{Q \cdot \Delta t}{\Delta V}(C_i^t - C_{i-1}^t) + [-k_a(1-\theta_i^t)C_i^t + k_d\theta_i^t] \cdot S \cdot \Delta t \quad (10)$$

ΔV is defined as:

$$\Delta V = \frac{LA_s - (W/\rho_p)}{n} \quad (11)$$

where W is the weight of adsorbent (kg); n is the entity of n series of constant volume unit ($n = 50$) and A_s is the cross sectional area of the adsorbent bed (m^2), respectively. Q is the flow rate of the feed containing VOC.

2.2. Measurement of adsorption capacity

The amount (weight) of VOC adsorbed at equilibrium adsorption is W_e .The equilibrium adsorption capacity, q_e is defined as:

$$q_e = \frac{W_e}{W} \quad (12)$$

At any time, t, the adsorption capacity q can be calculated from Eq. (13).

$$q = \int_0^t (C_o - C_{exit}) \cdot \frac{Q}{W} dt \quad (13)$$

where C_o and C_{exit} are obtained from experimental data and the value of q is obtained. The equilibrium adsorption capacity, q_e can also be calculated once equilibrium concentration of VOC is substituted in Eq. (13).

In numerical solution, a series of known (ρ_p, A_s, C_o, W, L, Q and T) and estimated (k_a and k_d) are given as input into Eqs. (9) and (10), respectively, followed by an iterative computations. The breakthrough curves are obtained theoretically. The best fit was verified by evaluating the root mean square error method, δ, from Eq. (14).

$$\delta = \frac{1}{C_o}\sqrt{\sum_{n=1}^{N}(C_{exit} - C_{cal})^2} \quad (14)$$

where $(C_{exit} - C_{cal})$ is the deviation between the experimental and calculated concentration at breakthrough. N is the number of measurements in each test.

3. Experimental

3.1. Adsorbent preparation

In present study, silver was loaded in the zeolite supports (Y with Si/Al = 40 and ZSM-5 with Si/Al = 140) using ion exchange and incipient wetness impregnation methods. In the preparation of silver ion-exchange zeolite, 10 g of zeolite powder was added to an $AgNO_3$ solution, 20 ml with 0.05 M solution/g of zeolite support. The mixture was then stirred at room temperature for 24 h. The ion exchange process was repeated until the maximum possible equilibrium exchange was achieved. The suspension was then filtered and dried at 80 °C, followed by calcination at 550 °C for 6 h. Silver-loaded zeolites were also prepared via incipient wetness impregnation method. In this procedure, 20 ml of 0.05 M $AgNO_3$ solution was added to 5 g of zeolite support. The slurry mixture was placed in a rotary evaporator and kept under vacuum at 100 °C to allow the slurry to dryness by water removal from the slurry. All the above-mentioned procedures were performed in dark to avoid any effect of light. The prepared adsorbent was then calcined at 550 °C for 6 h. Before the adsorbents were used in the adsorption column, they were converted into a 10 mm diameter pellet using 6 tonnes hydraulic pellet making press. The pellets were then crushed and sieved into particle size of between 250 and 300 μm.

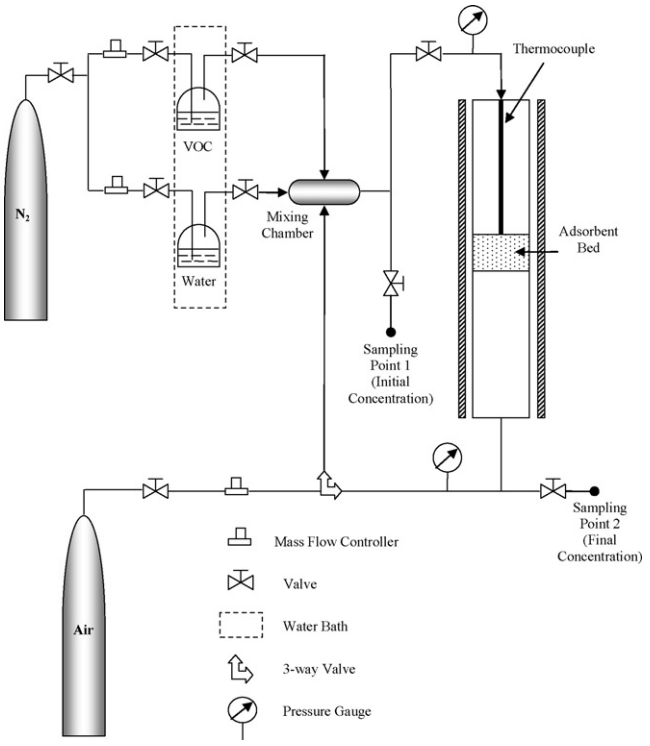

Fig. 1. Experimental setup for adsorption process study.

3.2. Experimental setup

Adsorption process studies were carried out using a 19 mm o.d. stainless steel column of 15 mm i.d. and 1000 mm length as shown in Fig. 1. A known amount of adsorbent was used to get the required GHSV. The temperature in the column was monitored and less than 5 °C temperature difference was observed within the column in the axial direction. The temperature was monitored with a K-type temperature probe interfaced to the unit control box. The process parameters for the adsorption study are presented in Table 1. The VOC uptake capacity, corresponding breakthrough time and saturation time were the main process parameters. The experiments were conducted under two different modes of operation in the

Table 1
Process parameters for adsorption studies

Process variables	Unit	Column operation mode	
		Dry feed	Humid feed
Weight of adsorbent	g	0.33; 0.85	0.33; 0.85
Feed flow rate	ml/min	150	165
GHSV	h^{-1}	5,000; 13,000	14,600
Feed VOC concentration	ppm	1,000; 4,500	1,000; 4,500
Relative humidity	%	0	35
Temperature	°C	28–30	28–30

Table 2
Silver-loaded zeolites prepared by ion exchange and impregnation methods

Catalyst	Notation	Si/Al ratio	Preparation method	Silver loading (wt%)
AgY	AgY(IE)	40	Ion exchange	2.5
AgY	AgY(IM)	40	Impregnation	22.4
AgZSM-5	AgZSM-5(IE)	140	Ion exchange	3.2
AgZSM-5	AgZSM-5(IM)	140	Impregnation	26.6

present study. The adsorbent performance measurements were conducted under the dry feed mode. Meanwhile, in order to study the effect of moisture towards the adsorbent activity, the nitrogen gas flow at 15 ml/min was used to bubble the heated distilled water in a constant temperature water bath at 30 °C. All the experiments were operated at room temperature. The adsorption data were taken at 10 min sampling interval to examine the adsorbent breakthrough until the adsorbent was saturated. The changes in the exit VOC concentration to the initial VOC concentration were monitored using gas chromatography. After reaching saturation of the adsorbent bed, the adsorbed VOC was desorbed using hot nitrogen gas at a flow rate of 50 ml/min. The heating rate of adsorbent was 5 °C/min.

3.3. Products analysis

The composition of the feed and product streams was analyzed using a Hewlett Packard, Model 5890 series II gas chromatograph (GC). The GC was equipped with a flame ionisation detector (FID). The chromatography column employed for the analysis of adsorption feed composition and products was a Porapak Q column (6 m long × 2.33 mm i.d.). Helium at a constant flow rate of 20 ml/min was used as the GC carrier gas. The GC oven temperature was maintained at 180 °C. These settings gave a maximum elution time of 20 min. The FID was interfaced to a Hewlett Packard 3396 Series II integrator. The peak areas of each individual component were used to calculate the mole fraction of each component. Generally, the standard errors and reproducibility of the experimental results reported in this manuscript are within ±5% or the reported values. Data points dropped outside this range were discarded and the measurement was repeated.

4. Results and discussion

4.1. Screening of adsorbents

Silver metal was chosen to be loaded on the zeolites in the present study as the end goal was to use the silver-zeolite for the combined adsorption–catalytic decomposition of VOC. However, the scopes of the present study are only limited to the adsorption process and its modelling. The presence of a metal on the zeolite support may modify the Brønsted acid sites of the zeolite [17] and further the metal state is influenced by the choice of the support. In order to quantify the total amount of silver incorporated in the adsorbent and the Si/Al ratio of the zeolite, inductive couple plasma (ICP) analysis was done and the results are presented in Table 2. It is noted in the table that ion exchange process resulted in adsorbents with significantly lower silver loadings. This was due to the limited number of exchange sites available in the zeolites while only physical deposition of metal crystallites was involved in the adsorbents prepared through impregnation method. However, changes in the adsorption behaviours were likely as some of the silver crystallites would deposit on pore mouths to influence the diffusion of adsorbate. Besides, it could cause the physical coverage of surface areas to significantly affect the adsorption process which is governed by surface phenomena.

Adsorption and desorption of butyl acetate were carried out in a fixed bed adsorption column charged with the four different adsorbents prepared. The breakthrough curves for each of 0.3 g adsorbent, resulting in a GHSV of 13,000 h^{-1} were obtained at room temperature. The adsorption capacities were determined by calculating the areas from the breakthrough curves. The inlet stream feed composition was a mixture of 1000 ppm of butyl acetate in air with a total flow rate of 150 ml/min.

The adsorption breakthrough curves for AgY and AgZSM-5 with different silver incorporation methods are shown in Fig. 2. AgY (IM) and AgZSM-5(IM) both reached the saturation after 20 min those adsorbents prepared trough an ion exchange process required at least 30 min before the significant increase in the butyl acetate in the outlet gas was detected. All adsorbents were considered to reach their adsorptive capacity after about 90 min when no net adsorption was observed. It is also observed in the figure that zeolite Y resulted in better adsorbents regardless of the metal incorporation methods. This was attributed to surface characteristics of this zeolite and its acidic nature as its Si/Al was significantly lower than that of ZSM-5 [3]. These results also suggest that impregnation was not a preferred method for silver introduction as far as the adsorption performance is concerned.

The inefficiency of the adsorption process for impregnated samples was deemed to result from the partial pore blockage of its pores by the silver particles. Canizares et al. [14] reported that the micropore surface area and the micropore volume were lower for the metal containing catalyst than those of metal free material

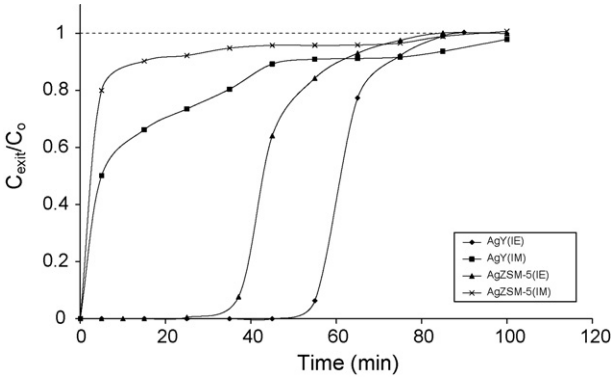

Fig. 2. Adsorption breakthrough curves for AgY(IE), AgY(IM), AgZSM-5(IE) and AgZSM-5(IM).

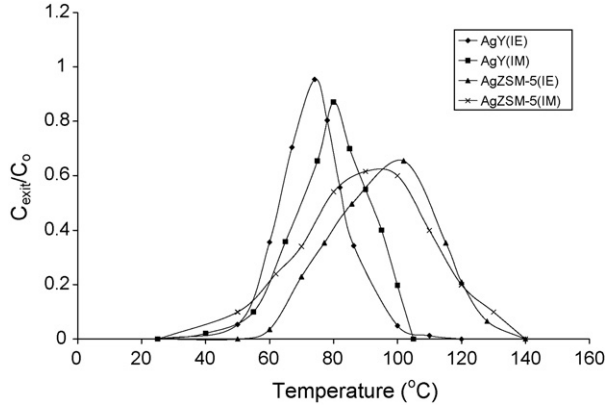

Fig. 3. Desorption of butyl acetate over AgY(IE), AgY(IM), AgZSM-5(IE) and AgZSM-5(IM).

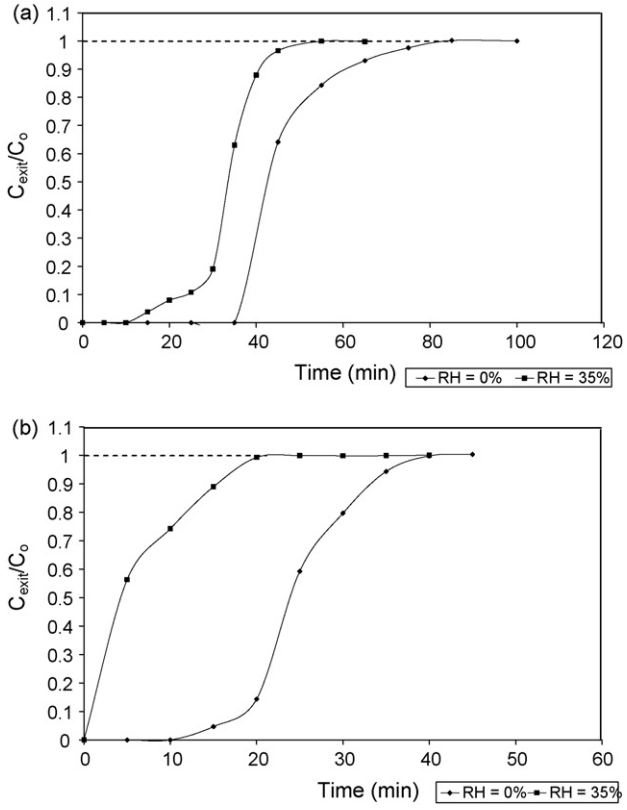

Fig. 4. Profile of breakthrough curve of butyl acetate on AgY(IE) for dry and humid feed stream for (a) GHSV = 13,000 h^{-1}; C_{voc} = 1,000 ppm and (b) GHSV = 5,000 h^{-1}; C_{voc} = 4500 ppm.

due to blocking of pores and subsequent drop in surface area and pore volume. The changes in surface area of the catalyst were attributed to the introduction of bigger cations in place of smaller Na^+ cation into the zeolite structure [17]. Baek et al. [3] prepared silver loaded on HY (80) with weight loadings varied from 0.5% to 22.4%. It was found that the surface area of the fresh prepared catalyst dropped from 678 to 322 m^2/g. During the adsorption process, VOC molecules come into contact with forces acting at the surface of the adsorbent to consequently attach to the surface as an adsorbed phase. Generally, the adsorption process is not dependent on the preparation method (ion-exchange or impregnation) of silver loadings but it depends on the physical and chemical characteristics that result. The higher surface area and pore volume generally results in the higher amount of the component to be adsorbed at equilibrium.

Adsorption of butyl acetate mainly occurred on the surface of the zeolites used rather than on the metal sites. Therefore, the characteristics of the surface would greatly influence the adsorption behaviour. The introduction of silver in the zeolites through ion exchange and impregnation was also found to influence the adsorption behaviour as it could change the physical and chemical properties of the materials as observed in this study. Different metal introduction method would result in different characteristics of the adsorbent which in turn, affect the adsorption process. However, the as the surface coverage by metal sites was much lower than that by the zeolitic surface, the more dominant effects on the adsorption process would still be caused by the type of zeolite used. In this study, Y zeolite-based materials were better adsorbents than that of ZSM-5, regardless of the preparation method used.

The isotherm of VOC adsorbed on zeolite Y present an S-shape which corresponds to Type V of the IUPAC classification. In contrast, the isotherms of VOC on ZSM-5 are more of Type I [18]. The adsorption useful domain of these isotherm classifications is the abrupt step which corresponds to the filling of micropores. S-shape isotherms of zeolite Y are not favourable to adsorption, but favourable for desorption and these behaviours are in contrast for Type I isotherm of ZSM-5. Therefore, zeolite Y would be more easily regenerated than ZSM-5 [19].

Fig. 3 shows the desorption results of different adsorbents prepared with ion exchange method and impregnation methods. The GHSV for the desorption test was fixed at 5000 h^{-1}. These profiles obtained correspond to the concentration of desorbed butyl acetate in the outlet gas when the saturated adsorbents were exposed to increasing temperature. The peaks for the desorption process at around 80 °C for AgY and at about 100 °C for AgZSM-5 was observed. This result clearly suggests the stronger interaction between the adsorbed butyl acetate and ZSM-5 surface. Despite showing higher adsorption capacity as suggested by results in Fig. 2, zeolite Y based adsorbents showed earlier desorption suggesting weaker interaction between them and the adsorbate. This observation was attributed to the higher number of sites responsible for adsorption but the interactions involved between the adsorbent-adsorbate were deemed to of weaker strength. The higher hydrophobicity of the ZSM-5 (at higher Si/Al ratio) was thought to be the responsible factor. This result also means the easier desorption of the organic from the adsorbent during the desorption step.

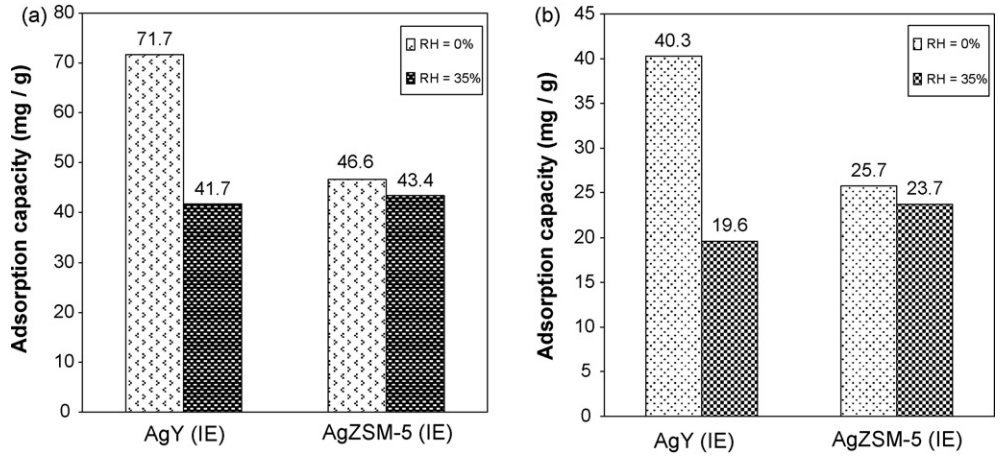

Fig. 5. Butyl acetate uptake by zeolite AgY(IE) and AgZSM-5(IE) at 28 °C: (a) GHSV = 5000 h^{-1}; C_{voc} = 4500 ppm and (b) GHSV = 5000 h^{-1}; C_{voc} = 1000 ppm.

Table 3
Adsorption capacity of butyl acetate onto AgY(IE) and AgZSM-5(IE) at 30 °C

Condition and results	Unit	Run 1	Run 2	Run 3	Run 4	Run 5	Run 6	Run 7	Run 8
AgY(IE)									
Concentration, C_o	ppm	4500	4500	4500	4500	1000	1000	1000	1000
Relative humidity, RH	%	0	35	0	35	35	0	35	0
Weight of adsorbent, W	g	0.33	0.33	0.85	0.85	0.33	0.85	0.85	0.33
Weight of butyl acetate adsorbed at equilibrium, W_e	g	19.67	6.86	60.95	35.45	10.73	33.66	34.26	10.40
Equilibrium adsorption capacity, q_e	mg/g	59.6	20.8	71.7	41.7	32.5	39.6	40.3	31.5
AgZSM-5(IE)									
Concentration, C_o	ppm	4500	4500	4500	4500	1000	1000	1000	1000
Relative humidity, RH	%	0	35	0	35	35	0	35	0
Weight of adsorbent, W	g	0.33	0.33	0.85	0.85	0.33	0.85	0.85	0.33
Weight of butyl acetate adsorbed at equilibrium, W_e	g	12.77	11.65	39.61	36.89	6.80	21.85	20.15	7.425
Equilibrium adsorption capacity, q_e	mg/g	38.7	35.3	46.6	43.4	20.6	25.7	23.7	22.5

4.2. Effect of moisture in the feed

The presence of moisture in the environment may influence the performance of adsorbent for butyl acetate adsorption. Delage et al. [10] concluded that the adsorption capacity is diminished significantly when the relative humidity of the VOC stream exceeds 50% and the VOC concentration is low. The effect of moisture is more prominent at lower VOC concentration and higher relative humidity involved [11]. Generally, the breakthrough of butyl acetate may take place earlier while the relative humidity of the air stream is increased as shown in Fig. 4(a) and (b). Both figures present the breakthrough rates at two relative humidity environments under various initial concentrations of VOC. The uptake of butyl acetate was quite competitive with water vapour as co-feed on the adsorbent surface and the adsorption capacity of the adsorbents were observed to drop when the humid feed was used. The effect was more pronounced when higher concentration of butyl acetate was used at lower GHSV. Regardless the throughput and the feed organic concentration, the similar behaviour observed in Fig. 4(a) and (b) strongly suggests the negative effect of moisture on the adsorption process.

The presence of water vapour in the gas stream containing butyl acetate caused the deflection of the breakthrough curve to be steeper as compared to the adsorption dry feed. Some adsorption sites which would adsorb butyl acetate vapour were initially occupied by water molecules and the adsorption capacity for VOC vapour was suppressed. This phenomenon was due to the preferential occupation of active sites by water vapour thereby dropping the number of adsorption active sites available for VOC molecules. The preference could be explained by considering the low Si/Al of zeolite Y (which is 40) that resulted in a material with lower hydrophobicity. Hence, the amount of adsorbed VOC decreased significantly.

Fig. 5 shows the comparison between the two silver-loaded zeolites AgY(IE) and AgZSM-5(IE) prepared using ion exchange for butyl acetate adsorption and co-adsorption of the VOC and water. The uptakes of butyl acetate in dry feed for AgY(IE) were 71.7 and 40.3 mg/g at the organic concentration of 4500 and 1000 ppm, respectively. These data suggested that the concentration of butyl acetate could influence the equilibrium reached. In comparison with AgZSM-5(IE), the maximum pure VOC uptake was only about 46 mg/g which occurred at the organic feed concen-

Table 4
Experimental conditions and adsorption parameters

Adsorption condition and parameters		Unit	Run 1	Run 2	Run 3	Run 4
AgY(IE)		Temperature (°C)	30	35	45	50
Experimental conditions	Gas hourly space velocity, GHSV	h^{-1}	13,000	13,000	13,000	13,000
	Breakthrough time, t_b	min	40	35	10	5
	Saturation time, t_e	min	100	90	45	35
	Weight of adsorbate (VOC) at equilibrium, W_e	g	10.40	9.37	7.90	6.53
Adsorption parameters	Equilibrium adsorption capacity, q_e	mg/g	31.5	28.4	23.6	19.8
	Adsorption rate constant, k_a	$m^3/(s\,mol)$	1.1×10^4	1.2×10^4	2.4×10^4	5.6×10^4
	Desorption rate constant, k_d	s^{-1}	75.9	103.5	300	1244.4
	Equilibrium constant, K	m^3/mol	145	116	80	45
Statistics	Convergence number, n	–	35	29	41	32
	Root mean square error, δ	–	0.05	0.04	0.02	0.07
Ag-ZSM-5(IE)						
Experimental conditions	Gas hourly space velocity, GHSV	h^{-1}	13,000	13,000	13,000	13,000
	Breakthrough time, t_b	min	35	30	15	10
	Saturation time, t_e	min	85	85	65	40
	Weight of adsorbate (VOC) at equilibrium, W_e	g	7.43	7.03	6.87	6.40
Adsorption parameters	Equilibrium adsorption capacity, q_e	mg/g	22.5	21.3	20.8	19.4
	Adsorption rate constant, k_a	$m^3/(s\,mol)$	2.2×10^4	2.4×10^4	2.98×10^4	4.73×10^4
	Desorption rate constant, k_d	s^{-1}	111.1	228.6	451.5	1182.5
	Equilibrium constant, K	m^3/mol	198	105	66	40
Statistics	Convergence number, n	–	27	35	24	40
	Root mean square error, δ	–	0.05	0.05	0.07	0.03

Note: $K = k_a/k$.

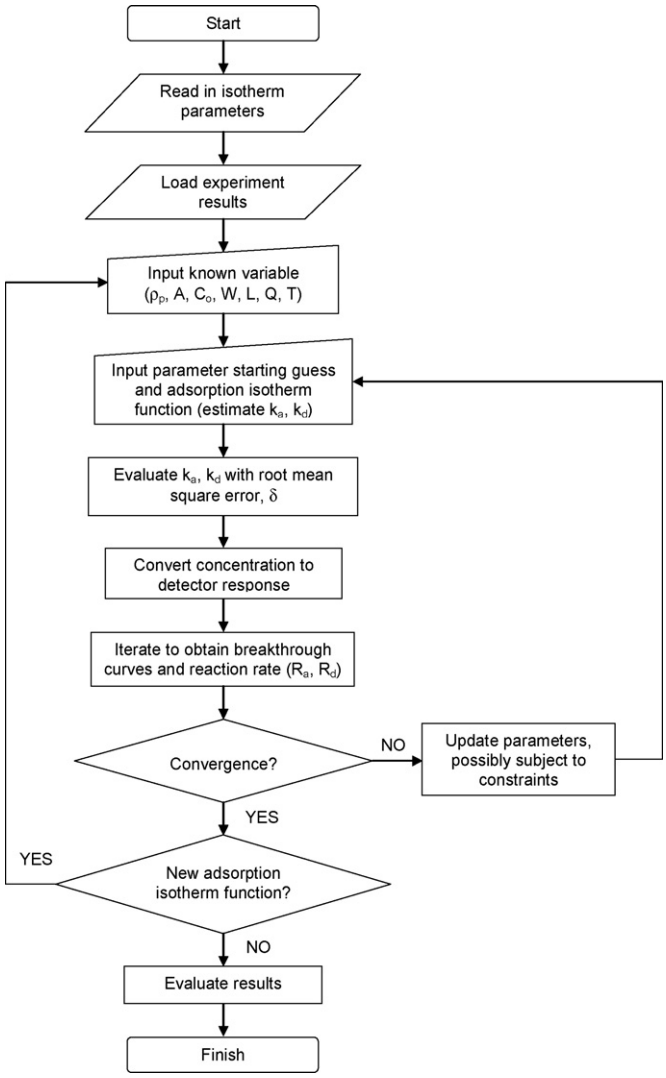

Fig. 6. Flow chart of algorithm for solving the adsorption model.

tration of 4500 ppm. Therefore, water uptake by AgZSM-5(IE) was found to be significantly lower than that by AgY(IE). Under humid feed, the performance of the ZSM-5 based adsorbent was actually slightly better than that of Y zeolite. These findings suggest the enhanced selectivity of the hydrophobic adsorbent AgZSM-5(IE) towards VOC.

These data shows that zeolite AgY(IE) was indeed a favourable adsorbent since AgY(IE) gave higher adsorption capacity for the tested VOC system. The behaviour was found to be unaffected by the feed organic concentration. However, the adsorption efficiency of AgY(IE) decreased by about 42% in the presence of water vapour as the co-feed. These results indicated that some of the zeolite adsorption sites were occupied by water. AgY(IE) may have both hydrophilic sites as well as hydrophobic sites. As AgY(IE) surface is less hydrophobic, the adsorbed water molecules on active sites act as nucleation sites for further adsorption of water and aggregates are formed as proved by the molecular simulation study by Müller et al. [20]. Hence, AgY(IE) may take up appreciable quantities of water thereby limiting their effectiveness for VOC control. The ionic nature of zeolites is also responsible for a high affinity for water [4]. The higher hydrophobicity of ZSM-5 at higher Si/Al ratio (140) could explain the relatively stable adsorption of the adsorbent under humid feed. Therefore, AgZSM-5(IE) gave an advantage in the application of VOC removal with relatively high humidity. The overall adsorption capacity was not much affected and it maintained the effectiveness with dry feed.

4.3. Adsorption capacities of adsorbents

Eq. (12) calculates the equilibrium adsorption capacity, q_e from the breakthrough data. The value q can be calculated from the Eq. (13) in which C_o and C_{exit} are inlet and outlet VOC concentration obtained at different times during the experimental run.

Table 3 summarizes the equilibrium adsorption capacity under various conditions. The amount of butyl acetate adsorbed at equilibrium was found to increase with an increase in the concentration of butyl acetate for both AgY(IE) and AgZSM-5(IE). This was attributed to the ability of butyl acetate to physically adsorb on the adsorbent as multiple layers [5]. As the butyl acetate concentration increased, the mass transfer zone was shortened so that a shorter time was required to reach the saturation. However, comparing the performance of both adsorbents, AgZSM-5(IE) generally gave lower adsorption capacity. As adsorption process belongs to the category of the diffusion-equilibration process on the surface, the larger surface area and pore volume will generally give higher capacity [21,22].

The weight of adsorbent was varied between 0.33 and 0.85 g with GHSV equivalent to 5000 and 13,000 h^{-1} at constant flow rate. Generally, the increase in amount of adsorbent induced the enhancement of adsorption capacity through increase of contacting probability. When the amount of adsorbent was increased, adsorption capacity showed maximum point for AgY(IE). This variation can be regarded to be constant for varying the amount if it is not too small or large. However, the adsorption on AgZSM-5(IE) did not show significant variation in the adsorbed amount at equilibrium with varying the amounts of adsorbent in the experimental range studied.

The adsorption capacity of butyl acetate adsorption on AgY(IE) in the present study was in the range of 59–71.7 mg/g. In a study by Wang et al. [23], the adsorption of butyl acetate was tested on three different adsorbents i.e. 13X zeolite, activated carbon and silica gel. They reported that the affinities between 13X zeolite and butyl acetate were lower than that with activated carbon and silica gel. The adsorption capacity on 13X zeolite, activated carbon and silica gel was 45, 966 and 554 mg/g, respectively. The given comparison shows that the present results are somewhat in the same order to the results published by Wang et al. [23].

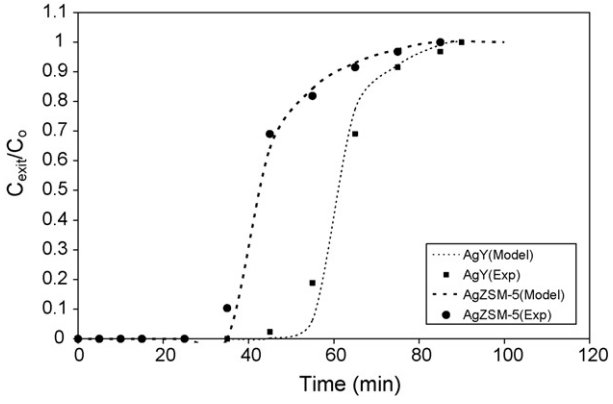

Fig. 7. Experimental and predicted breakthrough curves for butyl acetate on AgY(IE) and AgZSM-5(IE) (points are experimental data and lines are model predicted).

5. Adsorption column modelling

5.1. Adsorption rate parameters and equilibrium constant

Table 4 shows the experimental conditions and the results obtained for adsorption of butyl acetate on AgY(IE) and AgZSM-5(IE) at different temperatures. The model developed in the present study reasonably predicted the VOC concentration. The best fit was verified by root mean square error (δ) range from 0.02 to 0.07 [24]. It was observed that the equilibrium adsorption constant, K decreased drastically with the increase in temperature. At high temperatures, the adsorption capacity decreased relatively to small equilibrium constants and an early breakthrough time. The breakthrough curves were steeper at high temperature than low temperature due in part to the effect of k_a and k_d. Hence, high adsorption temperature has resulted in a steeper breakthrough curve; earlier breakthrough time. When the temperature increased from 30 to 50 °C and at an inflow concentration of 1000 ppm, the uptake of butyl acetate on AgZSM-5(IE) was reduced by 14% only, while that on the AgY(IE) was decreased by 37%. AgZSM-5(IE) was more hydrothermal stable and AgY(IE) was found to be temperature-dependant in compared with AgZSM-5(IE).

5.2. Breakthrough curves

Mathematical models presented in the form of partial differential equation for transient mass balance of butyl acetate in the solid and gas phase over an elemental section of an adsorption column were simulated using values of the input parameters presented in the flow chart of algorithm in Fig. 6. First, the experimental elution profiles were loaded. Then, the adsorption isotherm parameters were iteratively updated until the simulated and experimental profiles were close in agreement.

For prediction of the breakthrough curves, the numerical model approach was used. The column was divided into N equal increments ($\Delta z = 1/n$) and the convergence was studied by increasing the value of n. The calculated breakthrough curves converge when n was greater than 35. The simulation was carried out until n equal to 200 to ensure that there was no error due to numerical resolution of the system [24]. The main purpose of the approach developed in this work is that the parameters appearing in the model can be easily estimated from the correlations. Verification of the validity of the model has been attempted through comparison of the concentration histories measured at the end of the bed with those obtained from the proposed model. The simulated data versus experimental data gave good correlation coefficient and the root mean square error, δ were ± 0.05 for both AgY(IE) and AgZSM-5(IE) as shown in Fig. 7. It is clear from the figure that the simulated data agree well with the experimental data to indicate that the experimental data were accurately modelled. Similarly, the difference in the adsorption behaviour of AgY(IE) and AgZSM-5(IM) was successfully predicted with satisfactory accuracy.

6. Conclusions

1. Experimental adsorption studies of butyl acetate on AgY(IE) and AgZSM-5(IE) showed that equilibrium adsorption capacity of butyl acetate over AgY(IE) was higher. Mass transfer zone was well contained within the bed due to high affinity of both adsorbent for butyl acetate adsorption.
2. An early breakthrough and saturation were observed with higher inlet VOC concentration. The presence of moisture shifted the breakthrough of butyl acetate to take place earlier. The uptake of butyl acetate was quite competitive with water vapour as co-feed on the adsorbent surface and it caused the deflection of the breakthrough curve to be steeper as compared to the adsorption of pure VOC.
3. The adsorption efficiency of AgY(IE) dropped by about 42% in the presence of water vapour as co-feed. AgZSM-5(IE) gave an advantage in the application of VOC removal with relatively high humidity.
4. The adsorption model developed satisfactory fitted the experimental data for the prediction of adsorption parameters and equilibrium constant. The model was adequate to predict the adsorption and desorption behaviours between AgY(IE) and AgZSM-5(IE).

Acknowledgements

The authors would like to acknowledge the financial support from the Ministry of Science, Technology and Innovation of Malaysia (MOSTI) in the form of IRPA Grant (08-02-05-1039 EA 001) and that by the Universiti Sains Malaysia in the form of Research University (RU) grant to support this research project.

References

[1] D.M. Ruthven, Principle of Adsorption and Adsorption Processes, John Wiley & Sons, New York, 1984.
[2] L. Larrinaga, The SORBATHENE® Unit for Volatile Organic Vapour Recovery, Mississippi Technical Assistance Program, Southern States Annual Environmental Conference Biloxi, Mississippi, 1993.
[3] S. Baek, J. Kim, S. Ihm, Design of dual functional adsorbent/catalyst system for the control of VOC's by using metal-loaded hydrophobic Y-zeolites, Catal. Today 93–95 (2004) 575–581.
[4] W.J. Thomas, B. Crittenden, Adsorption Technology and Design, Butterworth-Heinemann, UK, 1998.
[5] E.C. Moretti, Practical Solutions for Reducing Volatile Organic Compounds and Hazardous Air Pollutants, American Institute of Chemical Engineers, New York, 2001.
[6] A.K. Ghoshal, S.D. Manjare, Selection of appropriate adsorption technique for recovery of VOCs: an analysis, J. Loss Prevent. Proc. Ind. 15 (2002) 413–421.
[7] C.T. Hsieh, J.M. Chen, Adsorption energy distribution model for VOCs onto activated carbons, J. Colloid Interf. Sci. 255 (2002) 248–253.
[8] M. Popescu, J.P. Joly, J. Carré, C. Danatoiu, Dynamical adsorption and temperature-programmed desorption of VOCs (toluene, butyl acetate and butanol) on activated carbons, Carbon 41 (2003) 739–748.
[9] W.H. Tao, T.C.K. Yang, Y.N. Chang, L.K. Chang, T.W. Chung, Effects of moisture on the adsorption of volatile organic compounds by zeolite 13X, J. Environ. Eng. 130 (10) (2004) 1210–1216.
[10] F. Delage, P. Pascaline, P.L. Cloirec, Effects of moisture on warming of activated carbon bed during VOC adsorption, J. Environ. Eng. 125 (12) (1999) 1160–1167.
[11] M. Chou, J. Chiou, Modelling effects of moisture on adsorption capacity of activated carbon for VOCs, J. Environ. Eng. 123 (5) (1997) 437–443.
[12] E. Biron, M.J.B. Evans, Dynamic adsorption of water-soluble and insoluble vapours on activated carbon, Carbon 36 (7) (1998) 1191–1197.
[13] M. Guillemot, J. Mijoin, S. Mignard, P. Magnoux, Volatile organic compounds (VOCs) removal over dual functional adsorbent/catalyst system, Appl. Catal. B 75 (2007) 249–255.
[14] P. Canizares, A.D. Lucas, F. Dorado, A.D. Asencio, Characterization of Ni and Pd supported on H-modernite catalysts: Influence of the metal loading method, Appl. Catal. A 169 (1998) 137–150.
[15] S. Lambert, C. Cellier, E.M. Gaigneaux, J.P. Pirard, Ag/SiO_2, Cu/SiO_2 and Pd/SiO_2 cogelled xerogel catalysts for benzene combustion: Relationship between operating synthesis variables and catalytic activity, Catal. Commun. 8 (8) (2007) 1244–1248.
[16] K. Yokozaki, H. Ono, A. Ayame, Kinetic hydrogen isotope effects in ethylene oxidation on silver catalysts, Appl. Catal. A 335 (1) (2008) 121–136.
[17] J. Zhou, Y. Zhang, X. Guo, W. Song, H. Bai, A. Zhang, Removal of C_2H_4 from a CO_2 stream by adsorption: A study in combination of *abinitio* calculation and experimental approach, Energy Fuels 20 (2006) 778–782.
[18] B. Clausse, B. Garrot, C. Cornier, C. Paulin, M. Simonot-Grange, F. Boutros, Adsorption of chlorinated volatile organic compounds on hydrophobic faujasite: correlation between the thermodynamic and kinetic properties and the prediction of air cleaning, Micropor. Mesopor. Mater. 25 (1998) 169–177.
[19] G. Delahay, B. Coq, Pollution abatement using zeolites: state of the art and further needs, Catal. Sci. Ser. 3 (1) (2001) 345–374.

[20] E.A. Müller, L.F. Rull, L.F. Vega, K.E. Gubbins, Adsorption of water on activated carbon: A molecular simulation study, J. Phys. Chem. 100 (4) (1996) 1189–1196.
[21] C. Tien, Adsorption Calculations and Modeling, Butterworth-Heinemann, Washington, 1994.
[22] H. Roohi, M. Azarpour, Adsorption of methanol on nanocrystalline H-zeolite and alkali metal-exchanged H-zeolites: energetic, NBO and QTAIM analyses, Micropor. Mesopor. Mater. 113 (2008) 343–351.
[23] C. Wang, T. Chung, C. Huang, H. Wu, Adsorption equilibria of acetate compounds on activated carbon, silica gel and 13X zeolite, J. Chem. Eng. Data 50 (2005) 811–816.
[24] S.D. Manjare, A.K. Ghoshal, Studies on dynamic adsorption behaviour of ethyl acetate from air on 5A and 13X molecular sieves, Can. J. Chem. Eng. 83 (2005) 232–241.